

# UC Irvine

## UC Irvine Previously Published Works

### Title

Evolution from insulator ( $x=0.003$ ) to metal ( $x=1$ ) of the  $\text{Eu}^{2+}$  local environment in  $\text{Ca}_{1-x}\text{Eu}_x\text{B}_6$

### Permalink

<https://escholarship.org/uc/item/0qv325m6>

### Journal

Journal of Applied Physics, 97(10)

### ISSN

0021-8979

### Authors

Urbano, RR  
Pagliuso, PG  
Rettori, C  
[et al.](#)

### Publication Date

2005-05-15

### DOI

10.1063/1.1855612

### License

[CC BY 4.0](#)

Peer reviewed

# Evolution from insulator ( $x=0.003$ ) to metal ( $x=1$ ) of the $\text{Eu}^{2+}$ local environment in $\text{Ca}_{1-x}\text{Eu}_x\text{B}_6$

R. R. Urbano,<sup>a)</sup> P. G. Pagliuso, and C. Rettori  
*Instituto de Física "Gleb Wataghin," Unicamp, 13083-970, Campinas, São Paulo, Brazil*

P. Schlottmann, S. Nakatsuji, and Z. Fisk  
*Department of Physics and National High Magnetic Field Laboratory, Florida State University, Tallahassee, Florida 32306*

J. L. Sarrao and A. Bianchi  
*Los Alamos National Laboratory, Los Alamos, New Mexico 87545*

S. B. Oseroff  
*San Diego State University, San Diego, California 92182*

(Presented on 8 November 2004; published online 2 May 2005)

The local environment of  $\text{Eu}^{2+}$  ( $4f^7$ ,  $S=7/2$ ) in  $\text{Ca}_{1-x}\text{Eu}_x\text{B}_6$  ( $0.003 \leq x \leq 1.00$ ) is studied by means of electron spin resonance (ESR). For  $x \leq 0.07$  the resonances have Lorentzian line shape, indicating an *insulating* environment for the  $\text{Eu}^{2+}$  ions. For  $x \geq 0.07$ , the lines broaden and become Dysonian in shape, suggesting a change to *metallic* environment for the  $\text{Eu}^{2+}$  ions, anticipating the *semimetallic* character of  $\text{EuB}_6$ . The broadening is attributed to a spin-flip scattering relaxation process due to the exchange interaction between conduction and  $\text{Eu}^{2+}4f$  electrons. High field ESR measurements for  $x \geq 0.30$  reveal narrower and anisotropic linewidths, which are attributed to magnetic polarons and Fermi surface effects, respectively. © 2005 American Institute of Physics. [DOI: 10.1063/1.1855612]

## I. INTRODUCTION

$\text{Ca}_{1-x}\text{R}_x\text{B}_6$  ( $R$ =rare earths, specially La) has become the focus of extensive investigations since the reported weak ferromagnetism (WF) at high  $T$  ( $T_c \approx 600$ – $800$  K).<sup>1</sup> Efforts were devoted, both, theoretically<sup>2–4</sup> and experimentally<sup>1,5</sup> to establish the origin of this WF in  $\text{Ca}_{1-x}\text{La}_x\text{B}_6$  and its relationship with the conducting nature of  $R$  doped  $\text{CaB}_6$ . Studies of the de Haas–van Alphen effect, the plasma edge in optical spectroscopy and the electrical resistivity support a semimetallic character for  $\text{CaB}_6$ , whereas NMR, angle-resolved photoemission (ARPES), thermopower, and other resistivity measurements suggest that  $\text{CaB}_6$  is a well defined semiconductor. High-resolution ARPES revealed an energy gap of  $\sim 1$  eV between the valence and conduction bands and a carrier density of the order of  $\sim 5 \times 10^{19} \text{ cm}^{-3}$  for  $\text{CaB}_6$  single crystals. Depending on the crystal growth method,  $\text{CaB}_6$  can also show WF and self-doping due to defects. The data for  $\text{Ca}_{0.995}\text{La}_{0.005}\text{B}_6$  are strongly sample dependent and doubts about the intrinsic nature of the WF in these systems have been raised. It has been suggested that  $\text{CaB}_6$  is a  $\sim 1$  eV gap semiconductor and that the intrinsic WF is hidden by the ferromagnetism (FM) of Fe and Ni impurities at the surface of the crystals.<sup>6</sup>

In contrast to  $\text{CaB}_6$ ,  $\text{EuB}_6$  is a well established *semimetallic* material that orders FM at  $T_c \approx 15$  K.<sup>7</sup> The substitution of  $\text{Ca}^{2+}$  by  $\text{Eu}^{2+}$  impurities breaks the translational invariance of the lattice and introduces localized split-off states from the valence/conduction band. The energy of such state lies in the gap of the semiconductor and its spatial extension is of the

order of one unit cell. An impurity band forms when the Eu bound states overlap, leading to an *insulator to metal* transition when a *percolative* network of impurity bound states is formed. This transition is revealed by the electron spin resonance (ESR) line shape.

Probing the local environment of  $\text{Eu}^{2+}$  via ESR sheds light on the magnetic/nonmagnetic and metallic/nonmetallic properties of  $\text{Ca}_{1-x}\text{Eu}_x\text{B}_6$ . We present systematic  $\text{Eu}^{2+}$  ESR measurements in single crystals of  $\text{Ca}_{1-x}\text{Eu}_x\text{B}_6$  for  $0.003 \leq x \leq 1.00$ . For  $\text{EuB}_6$  ( $x=1.00$ ) the broad ESR linewidth,  $\Delta H$ , was attributed to a spin-flip scattering relaxation due to the exchange interaction between the  $\text{Eu}^{2+}4f$  and conduction electrons.<sup>7</sup> The observed  $H$ ,  $T$ , and angle dependence of  $\Delta H$  is then intimately related to the formation of magnetic polarons and the Fermi surface of the conduction states.

## II. EXPERIMENTS

Single crystals of  $\text{Ca}_{1-x}\text{Eu}_x\text{B}_6$  ( $0.003 \leq x \leq 1.00$ ) were grown as in Ref. 1. The structure and phase purity were determined by x-ray powder diffraction and the crystal orientation by Laue x-ray diffraction. Most of the ESR experiments were carried out on  $\sim 1 \times 0.5 \times 0.3 \text{ mm}^3$  single crystals in a Bruker spectrometer using a X-band (9.48 GHz) TE<sub>102</sub> room- $T$  cavity and a Q-band (34.48 GHz) cool splitting cavity, both coupled to a  $T$  controller using a helium gas flux system for  $4.2 \leq T \leq 300$  K. The  $\text{Eu}^{2+}$  concentration was obtained from Curie–Weiss fits of the susceptibility data.

## III. RESULTS AND DISCUSSION

The room- $T$  X-band ESR spectra for  $H$  in the (110) plane along the angle of minimum  $\Delta H$ , i.e.,  $\sim 30^\circ$  ( $\sim 55^\circ$ ) away

<sup>a)</sup>Electronic mail: urbano@if.unicamp.br

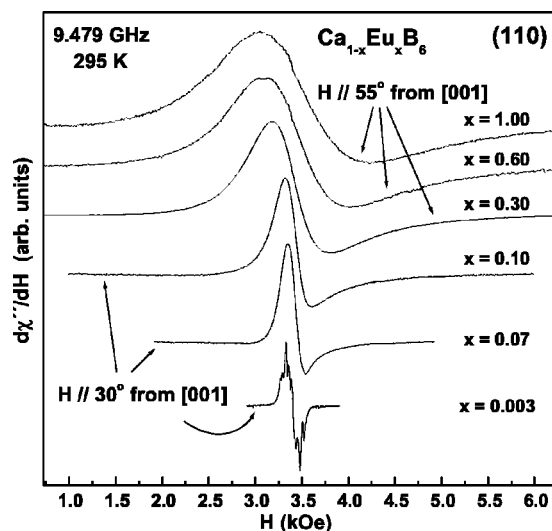


FIG. 1. ESR spectra of  $\text{Eu}^{2+}$  in  $\text{Ca}_{1-x}\text{Eu}_x\text{B}_6$  single crystals at room temperature with  $\mathbf{H}$  in the (110) plane. For  $0.003 \leq x \leq 0.10$   $\mathbf{H}$  is at  $30^\circ$  from [001], while for  $0.30 \leq x \leq 1.00$   $\mathbf{H}$  is at  $55^\circ$  from [001].

from the [001] direction for  $x \leq 0.10$  ( $x \geq 0.30$ ) is displayed in Fig. 1. The data show an increase of  $\Delta H$  as  $x$  increases. Around  $x \approx 0.07$  there is a crossover from Lorentzian to Dysonian line shape with an  $A/B$  ratio of  $\sim 2.3$  corresponding to a skin depth much smaller than the size of the crystals.<sup>8</sup> The Dysonian line shape suggests a *metallic* environment for the  $\text{Eu}^{2+}$  ions, confirming an increasing semimetallic character of  $\text{Ca}_{1-x}\text{Eu}_x\text{B}_6$  as  $x$  increases.

The angular dependence of  $\Delta H$  measured at X- and Q-band frequencies in the (110), (100) and (001) planes at 300 K and 50 K is presented in Fig. 2 for  $x=0.30$ . Note that

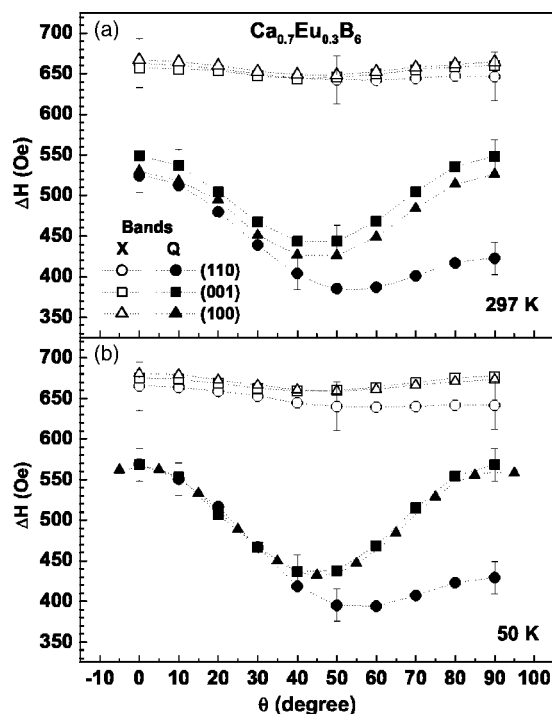


FIG. 2. Angular dependence of  $\Delta H$  for X band (open symbols) and Q band (closed symbols) in the (110), (001), and (100) planes for  $\text{Ca}_{0.7}\text{Eu}_{0.3}\text{B}_6$  at (a) room temperature and (b) 50 K.

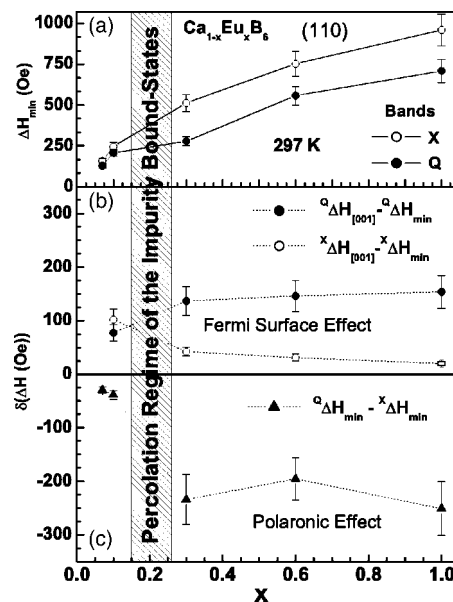


FIG. 3.  $H$  and  $x$  dependence of the ESR  $\Delta H$  at room temperature: (a) minimum linewidth at X and Q bands,  ${}^{X,Q}\Delta H_{\min}$ , (b) difference between the maximum and minimum linewidths,  ${}^{Q,X}\Delta H_{\text{[001]}} - {}^{Q,X}\Delta H_{\min}$ , and (c) difference between the minimum linewidths,  ${}^Q\Delta H_{\min} - {}^X\Delta H_{\min}$ . The *percolation* regime of the  $\text{Eu}^{2+}$  impurity bound states at  $0.10 \leq x \leq 0.30$  is shown as a shaded area.

$\Delta H$  is smaller and more anisotropic for high  $H$  (Q band). Above 50 K the anisotropy is independent of  $T$ .

$\Delta H$  for the spectra of Fig. 1 measured at X and Q bands is shown in Fig. 3(a). For  $x \geq 0.30$ , with the  $\text{Eu}^{2+}$  ions in the metallic environment,  $\Delta H$  becomes smaller at higher  $H$  (Q band). The larger anisotropy of  $\Delta H$ ,  ${}^{Q,X}\Delta H_{\text{[001]}} - {}^{Q,X}\Delta H_{\min}$ , for Q band than for X band is seen in Fig. 3(b). Figure 3(c) shows that the reduction,  ${}^Q\Delta H_{\min} - {}^X\Delta H_{\min}$ , is nearly  $x$  independent. This suggests that the dipolar interaction between  $\text{Eu}^{2+}$  ions cannot be the responsible mechanism for the broadening of the resonance as  $x$  increases.<sup>9</sup>

The ESR results of Fig. 1 for  $\text{Eu}^{2+}$  in  $\text{Ca}_{1-x}\text{Eu}_x\text{B}_6$  show three different concentration regimes. For  $x < 0.07$  the line shapes are Lorentzian, therefore, the local environment of the  $\text{Eu}^{2+}$  sites is *insulating*. In this regime the spectra show partially resolved fine structure and an overall minimum of  $\Delta H$  at  $30^\circ$  away from the [001] direction in the (110) plane.<sup>7</sup> For  $0.07 \leq x \leq 0.10$  the line shape starts to show an admixture of Lorentzian and Dysonian shape, i.e., it begins to display metallic character. For  $x \geq 0.30$  the line shape is pure Dysonian, i.e., the local environment is metallic with conduction electron spin diffusion.<sup>8</sup>

For small  $x$ , each  $\text{Eu}^{2+}$  represents a charge neutral substitution that, as a consequence of the broken translational invariance, gives rise to a bound state in the gap of the semiconductor. The impurity states are localized within the extension of about a unit cell. As the number of impurity states increases with  $x$ , they start to overlap, form a band, and eventually yield a percolative network. The critical concentration for nearest-neighbor site *percolation* on a simple cubic lattice is  $x_c = 0.307$ .<sup>10</sup> The percolation threshold is reduced to  $x_c = 0.137$  if next-to-nearest neighbors are included, which correspond to neighbors in the [110] directions. Third

neighbors are along the diagonals of the cube, but this direction is blocked for the wave functions because of the large  $B_6^{2-}$  anions. From our results in Fig. 1, it is reasonable to assume that the transition from *insulator* to *metal* occurs at  $x \approx 0.14$ . Hence, for  $x < x_c \approx 0.14$  the system is *insulating*. For  $x > x_c$ , the system is metallic and the spin diffusion of the conduction electrons gives rise to a Dysonian line shape. With increasing  $x$  the impurity band gradually smears the semiconducting gap and the system evolves to a *semimetal* for  $x=1$  ( $\text{EuB}_6$ ).<sup>7</sup>

For  $x \geq 0.30$ ,  $\Delta H$  has an overall cubic anisotropy corresponding to the superposition of three tetragonal environments [ $\Delta H_{\min}$  is at  $55^\circ$  in the (110), see Fig. 2]. This differs from the case for  $x \leq 0.07$  where the local symmetry is genuinely cubic. There are two possible scenarios to explain these findings. First, the origin for the tetragonal symmetry may be associated with the Eu/Ca substitution. This scenario assumes that the crystal field of an  $\text{Eu}^{2+}$  ion is determined by the nearest-neighbor cation ions. If a Eu ion is surrounded by five Eu and one Ca, the local symmetry is tetragonal. Since the Ca ion can be along any one of the axis, there is a superposition of tetragonal symmetries along the three directions. The overall spectrum is then cubic with inhomogeneous broadening. However, more than two Ca neighbors can give rise to a trigonal component in  $\Delta H$ , which was not observed. However, this mechanism does not account for the anisotropy observed in stoichiometric  $\text{EuB}_6$ .<sup>7</sup> It would require a much larger number of Eu vacancies than the claimed for these samples to explain the tetragonal dependence of  $\Delta H$ .<sup>11</sup>

The second possible scenario considers the relaxation of the  $\text{Eu}^{2+}$  spins into the conduction electron bath and the concomitant spin diffusion. The conduction electrons occupy small ellipsoidal pockets centered at the  $X$  points of the Brillouin zone, i.e., at  $(\pm\pi/a, 0, 0)$ ,  $(0, \pm\pi/a, 0)$ , and  $(0, 0, \pm\pi/a)$ ,<sup>12</sup> where  $a$  is the lattice constant. The drift of the diffusion is predominantly into the direction of the major axis of the ellipsoids, i.e., along one of the axes of the cube. Thus, each relaxation process gives rise to a tetragonal anisotropy of  $\Delta H$ . The superposition of the relaxation into the three directions is then expected. This mechanism explains why there is a tetragonal dependence in the metallic regime but not in the insulating one. The mechanism also applies to stoichiometric  $\text{EuB}_6$ .

$\Delta H$  for  $\text{EuB}_6$  was attributed to a homogeneous resonance with the main contribution to  $\Delta H$  involving spin-flip scattering relaxation due to the exchange interaction between the conduction and  $\text{Eu}^{2+}$   $4f$  electrons.<sup>7</sup> The  $H$ ,  $T$ , and angle de-

pendence of  $\Delta H$  suggests that magnetic polarons and Fermi surface effects dominate the spin-flip scattering in  $\text{EuB}_6$ . The second scenario is supported by the ESR and magnetoresistance data. Figures 2 and 3 show that the high- $H$  spectra have narrower lines for  $x \geq 0.30$ , indicating that the spin-flip mechanism is suppressed with field, which is consistent with the formation of polarons. This is similar to  $\text{EuB}_6$ . The negative magnetoresistance observed in  $\text{Ca}_{1-x}\text{Eu}_x\text{B}_6$  for  $x \geq 0.3$  also supports the presence of magnetic polarons.<sup>13</sup>

#### IV. CONCLUSIONS

The change in the line shape of the ESR spectra shows an evolution from insulating to semimetallic of the  $\text{Eu}^{2+}$  local environment in  $\text{Ca}_{1-x}\text{Eu}_x\text{B}_6$  as a function of  $x$ . The crossover between these two regimes is approximately in the range  $0.10 \leq x \leq 0.30$ . For  $x \geq 0.30$   $\Delta H$  shows: (i) a field narrowing, which is attributed to magnetic polarons,<sup>7</sup> and (ii) an overall cubic angular dependence corresponding to the superposition of three tetragonal components along the [001] axes, which is attributed to the relaxation mechanism and the Fermi surface.<sup>7</sup>

#### ACKNOWLEDGMENTS

This work was supported by FAPESP and CNPq, Brazil, and by US-NSF (Grant Nos. DMR-0102235 and DMR-0105431) and US-DOE (Grant No. DE-FG02-98ER45797). Work at the NHMFL was supported by NSF Cooperative Agreement No. DMR-9527035 and the State of Florida.

<sup>1</sup>D. P. Young *et al.*, Nature (London) **397**, 412 (1999).

<sup>2</sup>M. E. Zhitomirsky *et al.*, Nature (London) **402**, 251 (1999).

<sup>3</sup>H. J. Tromp *et al.*, Phys. Rev. Lett. **87**, 016401 (2000).

<sup>4</sup>S. Massidda, A. Continenza, T. M. de Pascale, and R. Monnier, Z. Phys. B: Condens. Matter **102**, 83 (1997).

<sup>5</sup>R. R. Urbano *et al.*, Phys. Rev. B **65**, 180407 (2002), and references therein.

<sup>6</sup>M. C. Bennett *et al.*, Phys. Rev. B **69**, 132407 (2004).

<sup>7</sup>R. R. Urbano, P. G. Pagliuso, C. Rettori, S. B. Oseroff, J. L. Sarrao, P. Schlottmann, and Z. Fisk, Phys. Rev. B **70**, 140401 (2004).

<sup>8</sup>G. E. Pake and E. M. Purcell, Phys. Rev. **74**, 1184 (1948); N. Bloembergen, J. Appl. Phys. **23**, 1383 (1952); G. Feher and A. F. Kip, Phys. Rev. **98**, 337 (1955); F. J. Dyson, *ibid.* **98**, 349 (1955).

<sup>9</sup>G. Sperlich and K. Jansen, Solid State Commun. **15**, 1105 (1974).

<sup>10</sup>J. W. Essam, in *Phase Transitions and Critical Phenomena*, edited by C. Domb and M. S. Green. (Academic, London, 1972), Vol. 2, p. 197; P. Schlottmann and C. S. Hellberg, J. Appl. Phys. **79**, 6414 (1996).

<sup>11</sup>Z. Fisk *et al.*, J. Appl. Phys. **50**, 1911 (1979).

<sup>12</sup>R. G. Goodrich, N. Harrison, J. J. Vuillemin, A. Tekul, D. W. Hall, Z. Fisk, D. Young, and J. Sarrao, Phys. Rev. B **58**, 14896 (1998).

<sup>13</sup>J.-S. Rhyee, B. K. Cho, and H.-C. Ri, Phys. Rev. B **67**, 125102 (2003); G. A. Wigger, C. Beeli, E. Felder, H. R. Ott, A. D. Bianchi, and Z. Fisk, Phys. Rev. Lett. **93**, 147203 (2004).

Journal of Applied Physics is copyrighted by AIP Publishing LLC (AIP). Reuse of AIP content is subject to the terms at: <http://scitation.aip.org/termsconditions>. For more information, see <http://publishing.aip.org/authors/rights-and-permissions>.